The temperature-programmed desorption of oxygen from an alumina-supported silver catalyst

G.W. Busser, O. Hinrichsen, and M. Muhler *
Ruhr-University Bochum, Laboratory of Industrial Chemistry, D-44780 Bochum, Germany

Received 22 November 2001; accepted 27 November 2001

The associative desorption kinetics of O_2 from a 15 wt% Ag/α-Al_2O_3 catalyst were studied under atmospheric pressure in a microreactor set-up by performing temperature-programmed desorption (TPD) experiments. Saturation with chemisorbed atomic oxygen (O$*$) was achieved by dosing O_2 for 1 h at 523 K and at atmospheric pressure followed by cooling in O_2 to room temperature. The TPD spectra showed almost symmetric O_2 peaks centred above 500 K, indicating associative desorption of O_2 from Ag metal surface sites. By varying the heating rates from 2 to 20 K min^{-1}, the O_2 TPD peak maxima were found to shift from 508 to 542 K, respectively. A microkinetic analysis of these TPD traces yielded an activation energy for desorption of 149 ± 2 kJ mol^{-1} and a corresponding pre-exponential factor of $2 \times 10^{12} \pm 1 \times 10^{12}$ s^{-1} in good agreement with the kinetic parameters reported for O_2 desorption under UHV conditions from Ag(111) and Ag(110) single crystal surfaces.

KEY WORDS: Ag/Al_2O_3 catalyst; temperature-programmed desorption; O_2 TPD.

1. Introduction

The interaction of oxygen with silver surfaces has been the subject of extensive research since silver is used as an unsupported catalyst for the selective oxidation of methanol to formaldehyde and as a supported catalyst for the epoxidation of ethylene [1–7]. One of the most important techniques applied to study this interaction quantitatively is temperature-programmed desorption [3,8–29].

In general, it is found that several oxygen species can exist on Ag surfaces. Molecular oxygen desorbs far below room temperature, whereas at higher temperatures the desorption of adsorbed atomic oxygen (O$*$) and atomic oxygen segregating out of the subsurface region and out of the bulk are observed. The objective of numerous studies was to correlate the presence of the different types of adsorbed oxygen species with the selectivity of the Ag catalysts. For instance, van Santen *et al*. [4] elegantly demonstrated the interaction of subsurface oxygen with O$*$ by performing TPD experiments with isotopically labeled oxygen.

Campbell *et al*. [11–13] used temperature-programmed desorption to derive the activation energy of associative desorption of O_2 from Ag(111) and Ag(110) single crystal surfaces using a pre-exponential factor of 10^{15} s^{-1} based on Langmuirian first-order desorption kinetics. Due to the low sticking coefficient of oxygen, relatively high dosing pressures (for UHV conditions, i.e. 5 mbar) had to be applied in order to achieve a high coverage of atomic oxygen structures such as the p(4×4)-O structure. However, this state could also be obtained by dosing NO_2 at much more moderate dosing pressures [16]. In a more recent study, Carlisle *et al*. [30] also reported on the interaction of oxygen with Ag(111). At very low oxygen coverages (below 0.05 ML) individual adatom adsorption was observed, whereas at higher coverages two-dimensional islands of Ag_2O were formed. Upon increasing exposure to NO_2, these islands were found to grow forming a well-ordered oxide film with a p(4×4)-O structure. Carlisle *et al*. [30] described the shape of the oxygen desorption peak as being remarkably narrow, which was attributed to the restructuring of the Ag surface during desorption. It was not possible to describe this phenomenon by a simple desorption mechanism. Also Raukema *et al*. [14,15] were not able to describe their TPD peak shapes with straightforward first- or second-order kinetics.

All of these studies were confined in most cases to unsupported, pure silver samples such as foils or single crystals, often under UHV conditions, whereas supported silver is the industrially important epoxidation catalyst. Therefore, in this contribution a detailed study is presented—for the first time to the best of our knowledge—in which the kinetic parameters of O_2 desorption from an Ag/Al_2O_3 catalyst under atmospheric pressure are derived from TPD experiments with different heating rates. Furthermore, a microkinetic analysis of the TPD data is performed allowing extrapolation to UHV conditions and assessment of the influence of readsorption.

* To whom correspondence should be addressed.
E-mail: muhler@techem.ruhr-uni-bochum.de

1011-372X/02/0400-0049/0

2. Experimental

The experiments were all carried out in a passivated stainless steel microreactor set-up, described in detail in reference [31], equipped with gas lines for He (purity 99.9999%) and O_2 (purity 99.995%). Gas analysis was performed by a calibrated quadrupole mass spectrometer (Balzers GAM 445). The kinetic experiments were carried out with a conventional Ag/Al_2O_3 catalyst (approx. 15 wt% Ag on α-Al_2O_3) prepared according to reference [7]. The resulting BET area was $1.9\,m^2\,g^{-1}$. In this study, 2.0 g of the 250–355 μm sieve fraction were filled into the reactor consisting of a glass-lined U-tube with an inner diameter of 8 mm resulting in a bed height of about 45 mm. In general, gas flow rates were $50\,N\,ml\,min^{-1}$ unless specified otherwise. All experiments were conducted with the same catalyst sample. The fresh catalyst contained a large amount of carbonaceous residues originating from the Ag precursor resulting in the desorption of CO, CO_2 and H_2O during the first TPD experiments. Therefore, the catalyst was subjected to a cyclic pretreatment consisting of flushing with pure O_2 at 523 K followed by a TPD experiment in order to check whether CO and CO_2 were still desorbing. After treating the catalyst in total for at least 6 h in O_2 at 523 K, the amounts of CO and CO_2 desorbing during a TPD experiment were found to be negligible. The subsequent TPD experiments were carried out according to the following procedure. The catalyst was treated with pure O_2 at 523 K for 1 h. Then, it was cooled in flowing O_2 below 323 K, and the gas mixture was switched to He in order to flush the reactor for at least 30 min to remove gas-phase O_2 completely. Subsequently, the O_2 desorption experiment was carried out by starting the temperature ramp up to 723 K. After the measurements, the catalyst was characterized using scanning electron microscopy (microscope: LEO 1530, GEMINI; analysis equipment: OXFORD ISIS).

3. Results

Figure 1 shows an SEM image and the silver particle size distribution determined from several SEM images of the catalyst after the treatment in pure O_2 at atmospheric pressure at 523 K. The silver particle size ranges from approximately 100 to 200 nm in good agreement with values reported in reference [7]. A silver surface area of about $0.39\,m^2\,g_{cat}^{-1}$ is estimated from the particle size distribution assuming a spherical particle shape.

Figure 2 displays the O_2 TPD traces obtained with different heating rates (β) after saturation with O$*$ by dosing O_2 at atmospheric pressure. The most pronounced feature is a rather symmetric peak centered at 542 K in case of $\beta = 20\,K\,min^{-1}$ (trace D) indicating associative O_2 desorption from metallic Ag surface sites. A closer inspection of trace D in figure 2 reveals that the desorption of O_2 from a second type of Ag site may contribute to the overall TPD profile leading to the weak shoulder at about 580 K. Furthermore, the desorption of O_2 is found to continue up to the end temperature of 723 K. The total amount of O_2 desorbing during the TPD experiments was obtained by integrating the TPD traces up to 723 K (table 1) yielding an average amount of $3.75\,\mu mol\,O_2\,g_{cat}^{-1}$.

Campbell [12] achieved a saturation coverage of $\Theta_O = 0.41$ on Ag(111) by dosing O_2 for 20 s at 490 K and at 5 Torr resulting in a p(4 $\times$ 4)-O structure. On Ag(110), a saturation coverage of $\Theta_O = 0.67$ was obtained by dosing O_2 for 20 s at 485 K and at 50 Torr leading to a c(6 $\times$ 2)-O structure [32]. Based on our results, a silver surface area of $0.79\,m^2\,g_{cat}^{-1}$ can be calculated assuming a mean site density of 1.15×10^{19} Ag atoms m^{-2} [33] and a mean surface stoichiometry of O$*$/Ag $= 1/2$. If one assumes the presence of a subsurface oxygen layer (*cf.* references [4,26]), a silver surface area of $0.40\,m^2\,g_{cat}^{-1}$ can be calculated. This value is in very good agreement with the value for the silver surface area determined from the SEM micrographs.

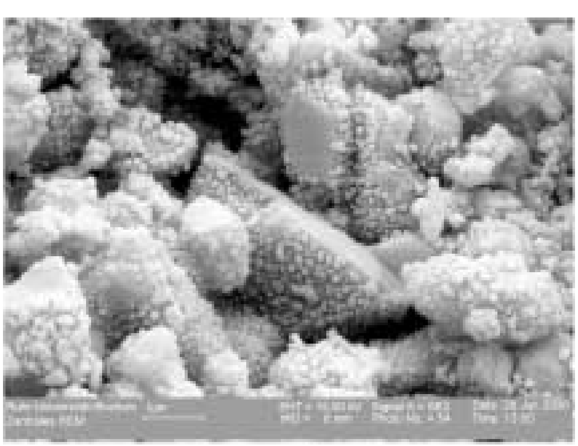

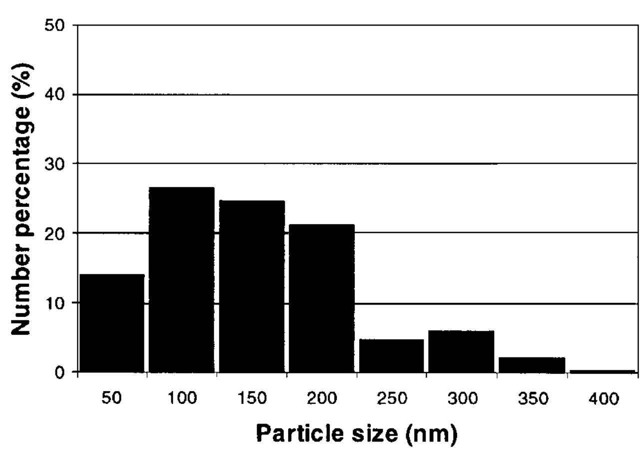

Figure 1. The Ag/Al_2O_3 catalyst after the pretreatment in flowing O_2 at atmospheric pressure: (left) SEM micrograph, (right) particle size distribution.

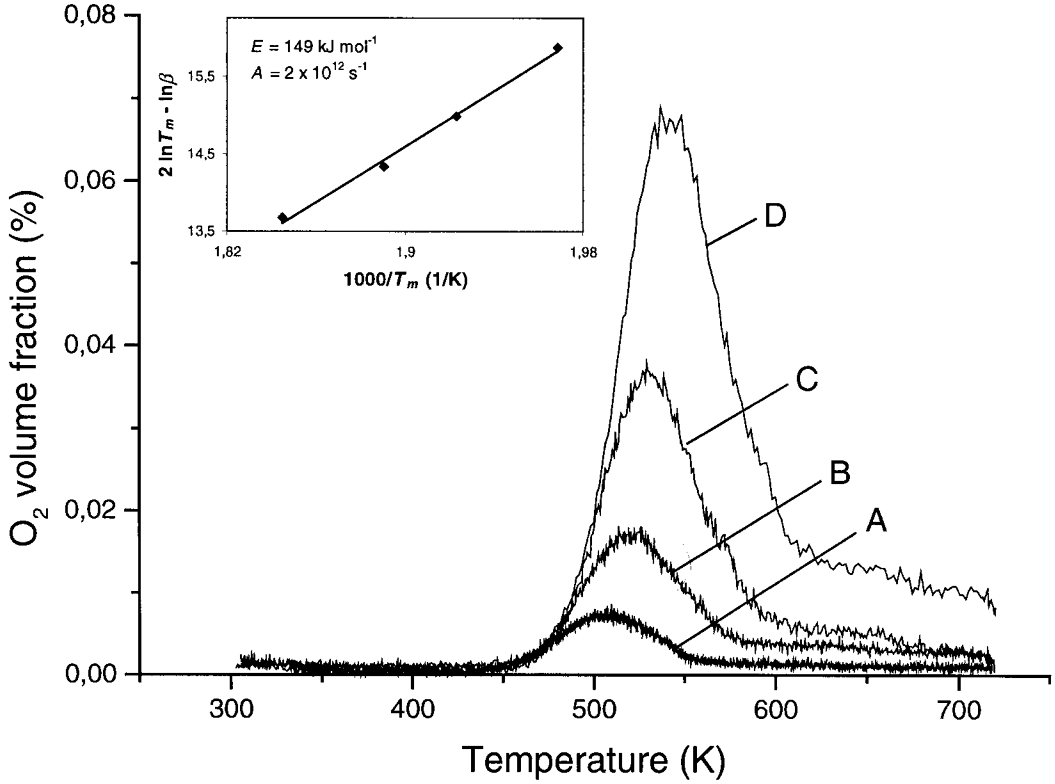

Figure 2. O_2 TPD spectra obtained after dosing O_2 at atmospheric pressure using the following heating rates: (A) 2 K min^{-1} ($T_{max} = 508$ K), (B) 5 K min^{-1} ($T_{max} = 520$ K), (C) 10 K min^{-1} ($T_{max} = 529$ K), (D) 20 K min^{-1} ($T_{max} = 542$ K). The inset shows the determination of the activation energy and pre-exponential factor from the heating rate variation assuming associative desorption without readsorption yielding a pre-exponential factor of 2×10^{12} s^{-1} and an activation energy of desorption of 149 kJ mol^{-1}.

The peak maximum temperature (T_{max}) shifts towards higher temperatures with increasing heating rates while the onset of the peaks remains at the same temperature of about 440 K. The full width at half maximum (FWHM) of about 67 K is constant for every TPD peak indicating the absence of readsorption and mass transport limitations. The determination of the activation energy of desorption and the corresponding pre-exponential factor is straightforward assuming second-order desorption without readsorption [34]. Plotting $\ln(T^2_{max}/\beta)$ *versus* $1/T_{max}$ results in a straight line as displayed in the inset of figure 2. Applying linear regression yields an activation energy of 149 ± 2 kJ mol^{-1} and a pre-exponential factor of $2 \times 10^{12} \pm 1 \times 10^{12}$ s^{-1} within the experimental errors.

For the simulation the microreactor was modeled as a

Table 1
The quantitative O_2 TPD results (peak maximum temperature T_{max}, amount of O_2 desorbed) obtained by varying the heating rate β

β (K/min)	T_{max} (K)	O_2 desorbed (μmol/g)
2	508	4.0
5	520	3.6
10	529	3.8
20	542	3.6

continuous stirred tank reactor (CSTR) combined with the differential equation for the associative desorption written in one step using a coverage-independent rate constant k. In the corresponding equation for the associative desorption from the Ag surface, $*$ denotes the active site:

$$2\mathrm{O}* \rightarrow \mathrm{O}_2 + 2* \tag{1}$$

$$r_{des} = k\Theta_O^2 = A\,\mathrm{e}^{(-E/RT)}\Theta_O^2. \tag{2}$$

Figure 3 shows the modeling results for a heating rate of 10 K min^{-1}. The parameters used ($A = 2 \times 10^{12}$ s^{-1}, $E =$ 147 kJ mol^{-1}, fractional coverage $\Theta_O = N/N_{max} = 1$) are those within the error bars derived from the TPD experiments with various heating rates. The onset of the modeled TPD profile, as well as the position of the peak maximum, are in very good agreement with the obtained experimental data. However, the comparison more clearly reveals that the experimental peak is not fully symmetric at higher temperatures, indicating the presence of a second type of adsorption site leading to the shoulder at about 570 K. The continuous desorption of O_2 at higher temperatures most probably results from oxygen diffusing out of the bulk which is not included in the model.

Although the interaction of O_2 with silver has been the subject of numerous studies, the kinetic parameters of O_2 desorption were only determined on Ag single crystal

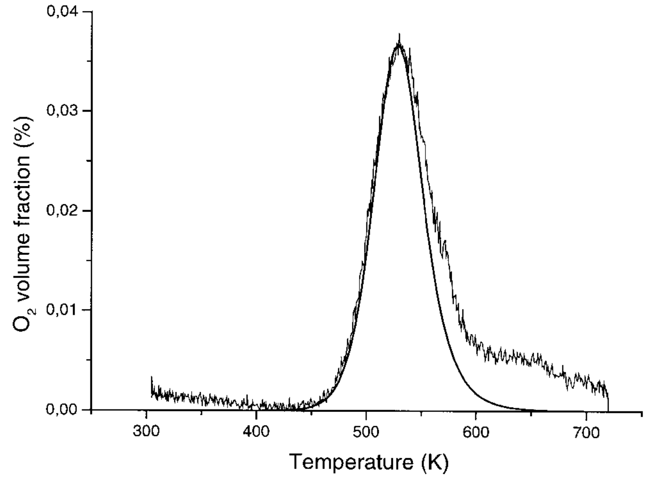

Figure 3. Modeling of the O_2 TPD trace (C) ($\beta = 10\,K\,min^{-1}$) based on the associative one-step mechanism using a pre-exponential factor of $2 \times 10^{12}\,s^{-1}$ and an activation energy of desorption of $147\,kJ\,mol^{-1}$.

surfaces. Campbell [12] derived the activation energy for oxygen desorption under UHV conditions using flash desorption from Ag(111) and Ag(110) based on a pre-exponential factor of $1 \times 10^{15}\,s^{-1}$ [35,36]. The reported kinetic data are summarized in table 2. In order to compare our data with those reported by Campbell, the O_2 TPD peak positions were calculated based on the one-step model using equations (1) and (2) with the kinetic parameters we obtained from the heating rate variation and the conditions which were applied by Campbell, i.e. UHV and a heating rate of $840\,K\,min^{-1}$. As a result, $T_{max} = 603\,K$ was obtained located between the value of T_{max} reported for Ag(111) and Ag(110), respectively. Campbell [12] observed that the desorption of O_2 from Ag(110) is accompanied with a restructuring of the adsorbate layer giving rise to two distinguishable peaks in the desorption spectrum, the low-temperature peak at 579 K being about half as high as the high-temperature peak at 617 K. Since we do not observe a second peak at lower temperatures, even though we applied a significantly higher O_2 dosing pressure compared with the pressures Campbell applied, we are more inclined to assign the symmetric TPD peak to associative O_2 desorption from Ag(111), for which a single symmetric O_2 TPD peak at 579 K is reported.

According to Campbell [12], a significant difference between Ag(111) and Ag(110) is the magnitude of the initial dissociative O_2 sticking coefficient which is two orders of magnitude lower on Ag(111) ($s_0 = 10^{-6}$) than on Ag(110) ($s_0 = 2 \times 10^{-4}$) at 490 K. The dissociative adsorption of O_2 occurs in two steps via the adsorption of molecular O_2 (k_{ads}) followed by dissociation (k_{dis}):

$$O_2 + * \underset{k_{dis}}{\overset{k_{ads}}{\rightleftharpoons}} O_2* \tag{3}$$

$$O_2* + * \underset{k_{rec}}{\overset{k_{dis}}{\rightleftharpoons}} 2O* \tag{4}$$

For the dissociation of adsorbed molecular O_2 on silver, he reports relatively low values of $E_{dis} = 34.7\,kJ\,mol^{-1}$ for Ag(111) and $E_{dis} = 32.6\,kJ\,mol^{-1}$ for Ag(110). The difference in dissociative sticking probability is therefore ascribed to the substantial difference in the pre-exponential factor for dissociation, which is a factor of 100 higher in case of Ag(110).

In order to study the possible influence of readsorption on the shape and position of the TPD peaks, the recombinative desorption of O_2 was modeled based on the two-step mechanism using equations (3) and (4). The set of start parameters is given in table 3, which is based on the parameters reported by Campbell for Ag(111) [12]. The following relation holds between A_{ads} and the initial sticking coefficient into the molecularly chemisorbed state s_M:

$$k_{ads} = A_{ads}\exp(-E_{ads}/RT) = \frac{s_M}{\sqrt{2\pi m k_B T}d} \tag{5}$$

with [12]

$$s_M = 0.25\exp(-E_{ads}/RT) \tag{6}$$

where k_B is the Boltzmann constant ($k_B = 1.38 \times 10^{-23}\,J\,K^{-1}$), m is the mass of oxygen ($m = 5.31 \times 10^{-26}\,kg\,mol^{-1}$), T is the temperature (K) and d is the density of sites ($d = 1.38 \times 10^{-19}\,m^{-2}$ for Ag(111) [12]).

In figure 4, traces A and B were obtained using the parameters reported by Campbell and the value for A_{ads} according to equation (5) at 400 and 600 K, respectively

Table 2
Kinetic parameters derived from Ag single crystal TPD studies (heating rate: $840\,K\,min^{-1}$; $\Theta_O = 0.4$–0.67). The activation energy of desorption E was derived using the Redhead equation based on $A = 10^{15}\,s^{-1}$ [12]

Single crystal surface	T_{max} (K)	E (kJ/mol)
Ag(111)	579	167
Ag(110)	617	178

Table 3
Set of starting parameters used in the calculation with the two-step mechanism; Ag(111) parameters obtained from reference [12]

Parameter	Value
E_{ads}	$13.4\,kJ\,mol^{-1}$
A_{ads} (400 K)	$421.9\,(Pa\,s)^{-1}$
A_{ads} (600 K)	$344.5\,(Pa\,s)^{-1}$
E_{des}	$51.9\,kJ\,mol^{-1}$
A_{des}	$1.0 \times 10^{13}\,s^{-1}$
E_{dis}	$34.7\,kJ\,mol^{-1}$
A_{dis}	$1.7 \times 10^{7}\,s^{-1}$
E_{rec}	$167\,kJ\,mol^{-1}$
A_{rec}	$1 \times 10^{15}\,s^{-1}$

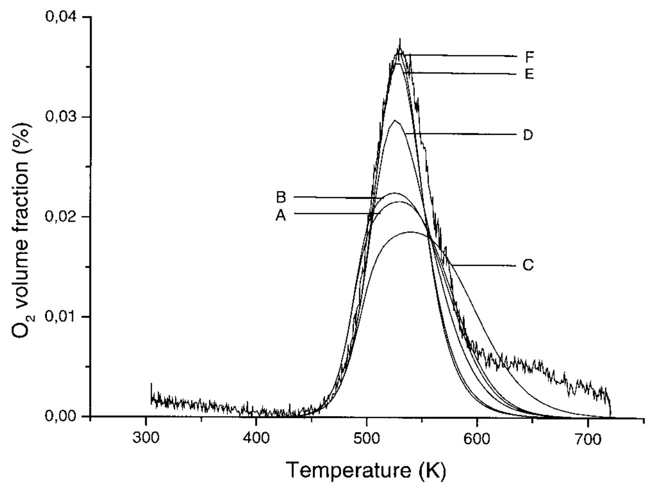

Figure 4. Modeling of the O_2 TPD trace (C) ($\beta = 10\,K\,min^{-1}$) based on the two-step mechanism. Trace (A) was obtained with the Ag(111) parameters as summarized in table 2 using A_{ads} (400 K); (B) as (A) with A_{ads} (600 K); (C) as (A) except for $A_{rec} = 2 \times 10^{12}\,s^{-1}$ and $E_{rec} = 147\,kJ\,mol^{-1}$; (D) as (C) except for $A_{dis} = 8.5 \times 10^5\,s^{-1}$; (E) as (C) except for $A_{dis} = 8.5 \times 10^4\,s^{-1}$; (F) as (C) except for $A_{dis} = 8.5 \times 10^3\,s^{-1}$.

(see table 3). It can be concluded that there is no significant difference between the two desorption patterns. This shows that the influence of the temperature on A_{ads} does not have a significant influence on the calculated pattern. Therefore, A_{ads} was set at the value calculated with $T = 400\,K$. The onset of the calculated desorption trace as well as the peak shape does not describe the experimental result very well. Trace C was calculated using the kinetic parameters of recombinative desorption (A_{rec}, E_{rec}) that were experimentally determined in this study from the variation of the heating rate. It can be concluded that, although the onset is in good agreement with the experimental result, the calculated TPD peak shape is far too broad to describe the experimental result. In order to decrease the influence of readsorption in the model the rate of dissociation was decreased by a factor of 10 leading to a narrower peak shape (trace D). When lowering r_{dis} even further by a factor of 100 (trace E) and 1000 (trace F), in fact resulting in an unreasonably low value, the modeled trace develops into a shape which is in very good agreement with the experimental data. However, the same result can be obtained when A_{ads} is decreased. Thus, we conclude that the overall process of dissociative adsorption of O_2 on Ag/Al_2O_3 is a very slow step in the high-coverage regime reached in the present study by dosing O_2 at atmospheric pressure.

Several studies have focused on the experimental determination of the activation energy and heats of adsorption of oxygen on supported silver. Auroux and Gravelle [37] report average heats of formation of an oxygen monolayer at 473 K on Ag/SiO_2 catalysts in the range of 205 to $385\,kJ\,mol^{-1}$. The differential heats of oxygen adsorption were found to decrease as the amount of adsorbed oxygen increased [37]. Kondarides and Verykios [29] report three different oxygen adsorption activation energies on $Ag/\alpha\text{-}Al_2O_3$ of 4.2, 43.9 and $100.4\,kJ\,mol^{-1}$, attributed to the formation of atomically adsorbed oxygen, weakly held molecularly adsorbed species and of subsurface oxygen, respectively. On the same system, Badani and Vannice [38] measured oxygen heats of adsorption in the range of 159.0 to $188.3\,kJ\,mol^{-1}$. It is obvious that the reported values differ strongly. Further studies are in progress in our laboratory employing different oxygen dosing pressures and temperature-programmed adsorption experiments to unravel the oxygen adsorption kinetics.

4. Conclusions

The temperature-programmed desorption of O_2 from a supported Ag catalyst was studied in a microreactor flow set-up. The results can be described very well by second-order desorption kinetics. A microkinetic analysis of the TPD traces with different heating rates yielded an activation energy for desorption of $149 \pm 2\,kJ\,mol^{-1}$ and a corresponding pre-exponential factor of $2 \times 10^{12} \pm 1 \times 10^{12}\,s^{-1}$ in good agreement with the kinetic parameters reported for O_2 desorption from Ag(111) and Ag(110) single crystal surfaces under UHV conditions. Due to the absence of readsorption effects, the rate of dissociative adsorption of O_2 was estimated to be at least a factor of 1000 lower than the rate based on the initial dissociative sticking coefficient on Ag single crystals.

References

[1] L. Lefferts, J.G. van Ommen and J.R.H. Ross, Appl. Catal. 31 (1987) 291.
[2] X. Bao, M. Muhler, B. Pettinger, R. Schlögl and G. Ertl, Catal. Lett. 22 (1993) 215.
[3] A. Nagy and G. Mestl, Appl. Catal. A: General 188 (1999) 337.
[4] R.A. van Santen and C.P.M. de Groot, J. Catal. 98 (1986) 530.
[5] R.A van Santen and H.P.C.E. Kuipers, Adv. Catal. 35 (1987) 265.
[6] J.G. Serafin, A.C. Liu and S.R. Seyedmonir, J. Mol. Catal. A: Chemical 131 (1998) 157.
[7] B.K. Hodnett, *Heterogeneous Catalytic Oxidation. Epoxidation of Alkenes: Reactivity of Electrophilic Oxygen Species* (Wiley–VCH, Weinheim, 2000) ch. 6, p. 160.
[8] G. Rovida, F. Praseti, M. Maglietta and E. Ferroni, Surf. Sci. 43 (1974) 230.
[9] G. Rovida and F. Pratesi, Surf. Sci. 52 (1975) 542.
[10] C. Backx, C.P.M. de Groot and P. Biloen, Surf. Sci. 104 (1981) 300.
[11] C.T. Campbell and M.T. Paffett, Surf. Sci. 139 (1984) 396.
[12] C.T. Campbell, Surf. Sci. 157 (1985) 43.
[13] C.T. Campbell, Surf. Sci. 173 (1986) L641.
[14] A. Raukema, D.A. Butler and A.W. Kleyn, J. Phys.: Condens. Matter 8 (1996) 2247.
[15] A. Raukema, D.A. Butler, F.M.A. Box and A.W. Kleyn, Surf. Sci. 347 (1996) 151.
[16] S.R. Bare, K. Griffiths, W.N. Lennard, H.T. Tang, Surf. Sci. 342 (1995) 185.
[17] R.J. Ekern and A.W. Czanderna, J. Catal. 46 (1977) 109.

[18] S. Kagawa, M. Iwamoto, H. Mori and T. Seiyama, J. Phys. Chem. 85 (1981) 434.
[19] S. Kagawa, M. Iwamoto and S. Morita, J. Chem. Soc. Faraday Trans. I 78 (1982) 143.
[20] X. Bao and J. Deng, J. Catal. 99 (1986) 391.
[21] R. Haul and G. Neubauer, J. Catal. 105 (1987) 39.
[22] H. Schubert, U. Tegtmeyer and R. Schlögl, Catal. Lett. 28 (1994) 383.
[23] V.I. Bukhtiyarov, A.I. Boronin and V.I. Savchenko, J. Catal. 150 (1994) 262.
[24] V.I. Bukhtiyarov, I.P. Prosvirin and R.I. Kvon, Surf. Sci. 320 (1994) L47.
[25] V.I. Bukhtiyarov, V.V. Kaichev, E.A. Podgornov and I.P. Prosvirin, Catal. Lett. 57 (1999) 233.
[26] V.I. Bukhtiyarov and V.V. Kaichev, J. Mol. Catal. A: Chem. 158 (2000) 167.
[27] D. Tsiplakides and C.G. Vayenas, J. Catal. 185 (1999) 237.
[28] A.J. Nagy, G. Mestl, D. Herein, G. Weinberg, E. Kitzelmann and R. Schlögl, J. Catal. 182 (1999) 417.
[28] D.I. Kondarides and X.E. Verykios, J. Catal. 143 (1993) 481.
[30] C.I. Carlisle, T. Fujimoto, W.S. Sim and D.A. King, Surf. Sci. 470 (2000) 15.
[31] T. Genger, O. Hinrichsen and M. Muhler, Catal. Lett. 59 (1999) 137.
[32] C.T. Campbell and M.T. Paffett, Surf. Sci. 143 (1984) 517.
[33] J.R. Anderson and K.C. Pratt, *Introduction to Characterization and Testing of Catalysts* (Academic Press, New York, 1985).
[34] J.L. Falconer and J.A. Schwarz, Catal. Rev.-Sci. Eng. 25(2) (1983) 141.
[35] M. Bowker, Surf. Sci. 100 (1980) L472.
[36] M. Bowker, M.A. Barteau and R.J. Madix, Surf. Sci. 92 (1980) 528.
[37] A. Auroux and P.C. Gravelle, Thermochim. Act. 47 (1981) 333.
[38] M.V. Bandani and M.A. Vannice, Appl. Catal. A: General 204 (2000) 129.